A Closer Look at Particle Exchange in the Gulf Stream*

AMY S. BOWER

Woods Hole Oceanographic Institution, Woods Hole, Massachusetts

M. SUSAN LOZIER

Ocean Sciences Program, Duke University, Durham, North Carolina

(Manuscript received 26 April 1993, in final form 3 November 1993)

ABSTRACT

The trajectories of 95 isopycnal floats deployed in the Gulf Stream in the last decade have shown that a substantial amount of particle exchange takes place between the Gulf Stream and the surrounding fluid at the level of the main thermocline. This exchange is suggestive of significant cross-stream eddy mixing, but in order to accurately interpret the float exchange in terms of property exchange the location of float deployment was assessed relative to the strong potential vorticity front associated with the Gulf Stream. The basic result of this analysis is that most of the observed float exchange is not representative of *cross-frontal* exchange. At the level where a strong potential vorticity front is present, some fluid particles escape from the jet, but most of them stay on the same side of the front. In the deep main thermocline, significant particle exchange is observed between the Gulf Stream and fluid on both sides of the jet, but this exchange is indicative of particles circulating in a relatively homogeneous pool of potential vorticity and thus does not signify a cross-stream property flux. These characteristics of particle exchange in the Gulf Stream are found to be generally compatible with the results from a study of particle behavior in a quasigeostrophic eddy-resolving GCM.

1. Introduction

The Gulf Stream has long been recognized as one of the most energetic ocean currents. It flows northward between the Florida Straits and Cape Hatteras as a western boundary current, separates from the coast of North America near 36°N, and continues east to the Grand Banks as a midlatitude jet (Fuglister 1963; Worthington 1976). In its eastward extension, the Gulf Stream transports on the order of 150 Sv (Sv $\equiv 10^6$ m^3 s^{-1}), of which about 30 Sv is associated with the wind-driven circulation of the subtropical gyre. The remainder is part of two recirculation cells north and south of the current (Hogg 1992). Because the eastward flow of the Gulf Stream extends to near the ocean bottom, the current is a *dynamical* boundary between the anticyclonic subtropical gyre to the south and the cyclonic circulation to the north throughout the water column.

It is also well known that a strong *property* front is associated with the Gulf Stream in the upper ocean. Synoptic observations of temperature, salinity, nutrients, potential vorticity and other tracers show that strong, narrow [O(20 km)] gradients of these properties are aligned closely with the Gulf Stream path (Fuglister 1963; McDowell et al. 1982; Bower et al. 1985). The property front separates warm, saline, low potential vorticity water of subtropical origin from cooler, fresher, high potential vorticity water of subpolar origin.

In the last ten years, our view of the Gulf Stream has been expanded by observations of particle motion made with neutrally buoyant subsurface floats. Analyses of several hundred trajectories (lasting from one month to several years) have revealed an interesting feature of the Gulf Stream: in spite of the fact that the Gulf Stream is always present as a distinct feature of the North Atlantic circulation, fluid particles are continuously being expelled from the current and replaced by other fluid particles from the surroundings (Shaw and Rossby 1984; Owens 1984; Bower and Rossby 1989; Cushman-Roisin 1993). This fluid particle behavior is illustrated in Fig. 1, which shows the trajectories of four isopycnal RAFOS floats deployed in the Gulf Stream near 500 m depth northeast of Cape Hatteras. Even though these floats were deployed in the center of the current, (i.e., in the high-speed core) they all escaped from the current in less than 30 days (Bower and Rossby 1989). The trajectories are superimposed on maps of sea surface temperature that indicate the position of the Gulf Stream and warm and cold core

* Woods Hole Oceanographic Institution Contribution Number 8407.

Corresponding author address: Dr. Amy S. Bower, Woods Hole Oceanographic Institution, Woods Hole, MA 02543.

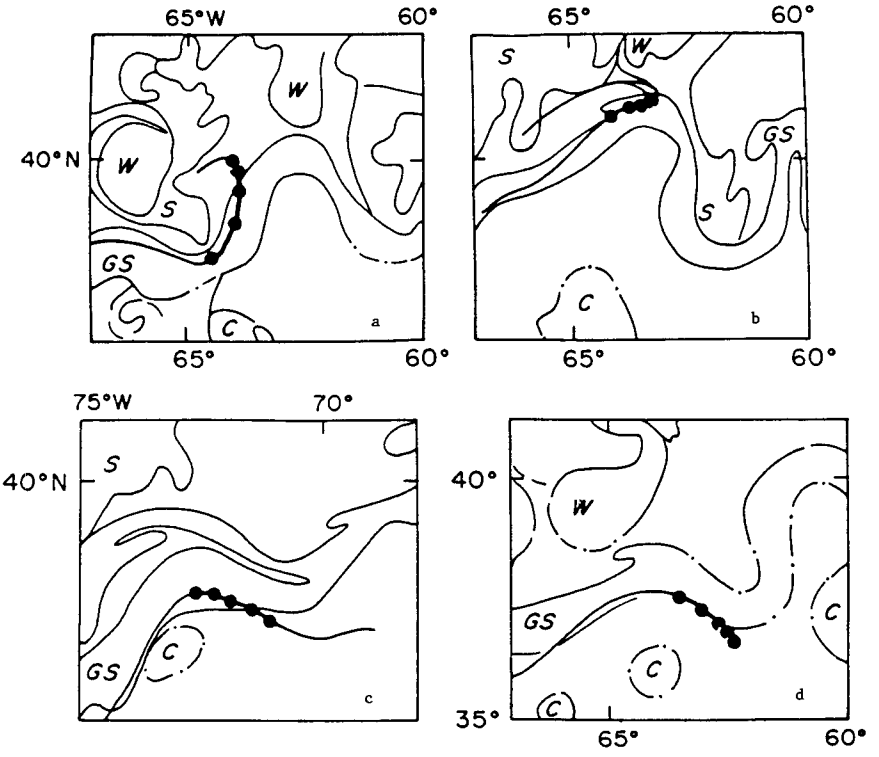

FIG. 1. Four examples of isopycnal RAFOS floats crossing out of the Gulf Stream superimposed on sea surface temperature (SST) field (GS: Gulf Stream, W: warm core ring, C: cold core ring). Dotted and dashed lines in SST field indicate that position of front is uncertain due to cloud cover or weak contrast. Dots on trajectories are 0000 UTC positions and leading two dots indicate position of the float when the SST satellite image was obtained. Note that the trajectories shown can span as many as 45 days, during which time the configuration of the stream path can change considerably. (a) RAFOS 10 (12°C surface); (b) RAFOS 52 (12°C surface); (c) RAFOS 21 (12°C surface); (d) RAFOS 35 (11°C surface).

rings at the time of each float passage. The dots on the trajectories show where the float was at the time the SST field was observed by satellite infrared imagery. In each of the four examples, the floats crossed out of the Gulf Stream as they approached meander crests or troughs. The escape of floats to the north (Figs. 1a and 1b) is clearly indicated by the deceleration of the float and the reversal in direction of the trajectory. Escape to the south (Figs. 1c and 1d) is evidenced by the rapid deceleration of the floats as they approach meander troughs. Some floats that escaped from the Gulf Stream were later reentrained into the current (not shown, see Bower and Rossby 1989).

Bower (1991) demonstrated that the entrainment and detrainment of fluid particles observed with the floats is related to the time-dependent propagation of meanders, which forces fluid particles to cross streamlines. The deviation of a particle trajectory from a given streamline depends on the difference between the particle's speed and the phase speed of the meanders. Particles moving rapidly compared to the phase speed of the meanders will not deviate substantially from a given streamline, but slower moving particles will experience significant departure from streamlines. Using typical Gulf Stream velocity profiles and meander phase speeds, Bower (1991) found that at the level where the floats shown in Fig. 1 were deployed, particles initially at the center of the jet can move to the edges of the jet and even escape altogether as a result of meander propagation.

While some aspects of the kinematics and dynamics of particle motion in the Gulf Stream have been studied in detail, an important question remains to be addressed; namely, does the observed *particle* exchange between the Gulf Stream and the surrounding fluid represent a significant *property flux* across the current? The study of cross-stream fluxes, and their signature in float trajectories, is motivated by modeling studies, which suggest that such fluxes may play a significant role in the maintenance of meridional distributions of oceanic properties, such as heat, salt, and potential vorticity. For example, studies of the ocean circulation based on eddy-resolving general circulation models (EGCMs) indicate that eddy potential vorticity fluxes across a midlatitude jet separating oppositely rotating, wind-driven gyres may be as important as western

boundary current dissipation in the basin-scale potential vorticity budget (Harrison and Holland 1981; Holland and Rhines 1980). In a study of a representative, three-layer quasigeostrophic EGCM, Lozier and Riser (1989) found that the majority of the potential vorticity imparted by the anticyclonic wind stress curl in the upper layer of the subtropical gyre was balanced by an eddy potential vorticity flux across the midlatitude jet rather than by dissipation along the western boundary. The ratio of frictional dissipation to eddy flux of potential vorticity depends on the frictional/inertial character of the model being considered (Lozier and Riser 1989), but these results certainly suggest that intergyre property fluxes could be important in the maintenance of property distributions in the ocean. Furthermore, Csanady (1989) has pointed out that the cross-stream eddy heat fluxes associated with the baroclinic instability of western boundary currents may be related to the energy cycle of the gyre-scale circulation.

Cross-stream eddy fluxes have been observed in the Gulf Stream, but their significance in the meridional balance of water properties has not yet been quantified. It has traditionally been thought that warm and cold core rings are responsible for most of the eddy property flux across the Gulf Stream. Rings form when meanders in the Gulf Stream's path grow to large amplitude and break off. The property front aligned with the Gulf Stream is similarly convoluted by the ring formation process, and a core of anomalous water is transported across the Gulf Stream. Their relatively large spatial scale, O(100–200 km), and their vivid presence in satellite infrared images of sea surface temperature have contributed to the reputation of rings as the primary flux mechanism. However, this concept has been challenged by the results of a study of cross-frontal eddy fluxes by Bower et al. (1985) based on the Gulf Stream '60 hydrographic survey. These authors found that rings were an order of magnitude less important than smaller scale, O(5–10 km) frontal mixing processes in the transport of dissolved oxygen across the Gulf Stream.

Trajectories of floats launched in the Gulf Stream have been quite useful for determining how fluid particles are exchanged between the Gulf Stream and the surrounding fluid. Based on the trajectories of 95 isopycnal RAFOS floats launched sequentially in the center of the Gulf Stream off Cape Hatteras, Bower and Rossby (1989) and Song et al. (1993) found that 69 floats escaped from the Gulf Stream before 30 days, and 62 of them did so by some mechanism *other* than the formation of new warm or cold core rings. To interpret this particle exchange as a signature of cross-stream mixing of properties we must first answer two fundamental questions. First, is there actually a property front at the level where these floats were deployed? Second, if a front is present at this level, are fluid particles moving across the front or are they moving in and out of the current while remaining on the same side of the property front?

In the present study, we address these questions by focusing on the isopycnal RAFOS floats mentioned above. These floats were deployed during two repeat-seeding experiments, the RAFOS Pilot Experiment (1984–85, Bower et al. 1986) and the RAFOS SYNOP Experiment (1988–90, Anderson-Fontana et al. 1991). In both of these programs, the floats were deployed sequentially in the Gulf Stream near the maximum in downstream speed about every 10 days, and tracked acoustically for up to 45 days. Fluid particles in the main thermocline, between the 7° and 17°C isotherms, were tagged.

To determine if the dispersion of floats is indicative of cross-stream exchange, it is necessary to know where the floats were launched relative to the front. For each float deployment, expendable bathythermographs (XBTs) were used to find the appropriate launch site for the floats, defined in terms of the thermal structure of the current. For the Pilot Experiment, this was the point where the 15°C isotherm intersected 400 m, and for the SYNOP Experiment, where 15°C intersected 450 m. This placed the floats in the high speed core of the jet (see Fig. 3). Usually only two or three XBTs were necessary to locate the launch site. Unfortunately, the location of the launch site within the larger-scale cross-stream structure of temperature, salinity, or potential vorticity cannot be determined from so few XBTs. We have therefore used an independent dataset to examine the location of the float launch site with respect to the property front in the Gulf Stream.

This dataset consists of 20 cross-stream sections of temperature and absolute velocity made across the Gulf Stream near the float launch site northeast of Cape Hatteras every two months between September 1980 and May 1983, using the free-falling velocity profiler, Pegasus (Halkin and Rossby 1985). For the purpose of this study we have chosen to define the front in terms of the potential vorticity gradient. Thus, our approach will be to use these data to construct sections of potential vorticity, and then, taking advantage of the fact that the RAFOS floats were always launched in the same location within the jet's thermal structure, we will determine where the float launch site was located relative to the potential vorticity front in each section. We will then be in a position to interpret the observed particle exchange in terms of cross-stream property flux.

Our analysis proceeds as follows. In section 2 we outline the method used to construct the potential vorticity sections from the Pegasus data. This is followed in section 3 by a description of the potential vorticity structure and the location of the RAFOS float launch site within that structure. In section 4, we discuss the interpretation of the float exchange and assess the compatibility of the observations with results from a quasigeostrophic EGCM. The work is summarized in section 5.

2. Methodology

a. The Pegasus dataset

The Pegasus cross sections consist of vertical profiles of velocity and temperature spaced every 25 km across the Gulf Stream with the number of stations per section varying from as few as four to a maximum of nine. The vertical resolution of the profiles is 25 m and nearly all the sections extend to at least 2000 m. To examine the cross-stream, rather than alongtransect, structure of the current, Halkin and Rossby transformed each of the sections into a streamwise coordinate system, where the downstream direction (y) at the time of each section was defined as the direction of the vertically averaged flow in the center of the jet.

b. Estimation of layer potential vorticity

To estimate potential vorticity from the Pegasus data, we have used a modified version of the procedure described by Leaman et al. (1989). These authors used *mean* sections of temperature and velocity, obtained with the Pegasus profiler at Cape Hatteras and at two upstream locations, to construct sections of *mean* potential vorticity in streamwise coordinates. In the present study, we have constructed *instantaneous* sections of potential vorticity from the bimonthly temperature (T) and downstream velocity (v) sections. We define isothermal layer potential vorticity (ILPV) in stream coordinates as an approximation of Ertel potential vorticity (Ertel 1942),

$$\mathrm{PV} = (2\vec{\Omega} + \vec{\zeta})\cdot\frac{\nabla\lambda}{\rho} \approx \frac{f + \partial v/\partial x}{H} = \mathrm{ILPV}, \quad (1)$$

where

$\vec{\Omega}$	angular velocity of the earth
$\vec{\zeta}$	relative vorticity of the fluid particle
λ	scalar property of the fluid particle (temperature in this case)
ρ	density
f	Coriolis parameter
$\partial v/\partial x$	cross-stream gradient of downstream velocity estimated *along* isothermal surfaces
H	thickness of layer bounded by two temperature surfaces.

This approximation is justified based on scaling analysis of the Ertel potential vorticity for the length and velocity scales of interest in the Gulf Stream (e.g., see Bower 1989). Curvature vorticity, part of relative vorticity in stream coordinates, is not included in Eq. (1). This omission will be addressed in the next subsection on errors and uncertainties.

Following the notation of Leaman et al. (1989), the layer boundaries were defined by $T_j = 27.0, 24.5, 22.0, 19.5, \cdots, 4.5$, with $\Delta T_j = T_j - T_{j+1} = 2.5°\mathrm{C}$. Layer thickness was estimated for the ith cross-stream position according to

$$H(x_i, \bar{T}_j) = z(x_i, T_j) - z(x_i, T_{j+1}), \quad (2)$$

where $\bar{T}_j = (T_j + T_{j+1})/2$. The average velocity within each layer was estimated by fitting a cubic spline to the vertical profile of velocity, integrating analytically between the layer boundaries and dividing by the layer thickness,

$$\bar{v}(x_i, \bar{T}_j) = \frac{1}{H(x_i, \bar{T}_j)} \int_{z(x_i,T_{j+1})}^{z(x_i,T_j)} v(x_i, z)dz. \quad (3)$$

The method used to estimate relative vorticity in the present study differs somewhat from that used by Leaman et al. (1989). They estimated $\partial\bar{v}/\partial x$ by taking the difference of estimates of $\bar{v}$ at neighboring stations and dividing by the station separation. In an effort to improve the estimate of horizontal shear, we have used cubic splines to estimate the cross-stream derivative of v at intervals of 10 km across the jet. This method was also used to interpolate thickness, H, at the same 10-km cross-stream grid points.

The interpolated values of H and $\partial\bar{v}/\partial x$ were used to calculate ILPV as a function of cross-stream distance and temperature. A constant value was used for the Coriolis parameter because f varies by only 2% across the stream [$\beta L/f = (2 \times 10^{-11}\ \mathrm{m^{-1}\ s^{-1}})(100\ \mathrm{km})/10^{-4}\ \mathrm{s^{-1}} = 0.02$].

c. Errors and uncertainties

The major uncertainties in this analysis fall into two categories: those associated with the estimation of potential vorticity and those associated with the fact that the RAFOS floats were not perfect isopycnal drifters. Regarding the estimation of potential vorticity, there are uncertainties associated with 1) the lack of curvature vorticity information, 2) measurement uncertainties in the basic data (temperature, pressure, and velocity), and 3) estimation of potential vorticity on isothermal rather than isopycnal surfaces. We address each of these sources of uncertainty individually, then we consider the isopycnal-following capability of the floats.

No observations of path curvature (κ) were made during the Pegasus experiment, precluding the estimation of curvature vorticity (κv). The meandering envelope of the Gulf Stream is narrow at Cape Hatteras, and curvature of the stream path is thus generally small, usually not exceeding 0.005 $\mathrm{km^{-1}}$ (radius of curvature: 200 km). Therefore, at the level of the main thermocline, where downstream speed is on the order of 100 cm $\mathrm{s^{-1}}$ or less, curvature vorticity is not more than 5% of f [$\kappa v/f = (0.005\ \mathrm{km^{-1}})(100\ \mathrm{cm\ s^{-1}})/10^{-4}\ \mathrm{s^{-1}} = 0.05$]. This suggests that curvature vorticity makes only a minor contribution to the total potential vorticity in the main thermocline. Nonetheless, for completeness, we have included a path curvature uncertainty of 0.005 $\mathrm{km^{-1}}$ in the uncertainty estimate for potential vorticity.

Halkin and Rossby (1985) reported uncertainties in the measurement of velocity and isotherm depth with the Pegasus instrument of 3 cm s^{-1} and 12 m. To evaluate the uncertainty in the estimate of shear vorticity due to the uncertainty in velocity, a Monte Carlo simulation was performed as follows (Press et al. 1988). For four representative velocity sections, several hundred cross-stream profiles of velocity were simulated by adding random noise to the original profiles from each layer. The noise was generated from a Gaussian probability distribution with a standard deviation of 3 cm s^{-1}, the uncertainty in the velocity measurement. Each of the simulated cross-stream profiles was then fit using a cubic spline. The horizontal derivative $(\partial\bar{v}/\partial x)$ of each simulation was calculated analytically from the spline, and the standard deviation of $\partial\bar{v}/\partial x$ based on all the simulated profiles was evaluated at each cross-stream location. The standard deviation was found to be quite uniform across each section and had a value of 0.19×10^{-5} s^{-1}, or about 2% of f. This value is based on an evaluation of all layers in the four representative sections, and is thus taken as the uncertainty in the estimate of $\partial\bar{v}/\partial x$ uniformly throughout all sections and layers. A similar procedure was carried out for the thickness data, and an uncertainty of 16 m in layer thickness was obtained.

Standard propagation of these measurement uncertainties leads to the following expression for the uncertainty in potential vorticity,

$$(\delta \text{ ILPV})^2 = \frac{(\delta\partial v/\partial x)^2 + (v\delta\kappa)^2}{H^2} + \frac{(\delta H)^2(f + \partial v/\partial x)^2}{H^4}, \quad (4)$$

where δX refers to the uncertainty in the estimate of quantity, X. Given constant values for the uncertainties as discussed above, Eq. (4) indicates that the uncertainty in potential vorticity is a function of potential vorticity and layer thickness. The largest uncertainties will be found where layer thickness is small and potential vorticity is large, such as in the cyclonic shear zone of the upper Gulf Stream. As will be seen in section 3, the uncertainty in potential vorticity throughout the main thermocline is less than about 30%.

We next consider the uncertainty associated with estimating potential vorticity along isothermal rather than isopycnal surfaces. Since fluid particle motion (and the float motion) is, to first order, along surfaces of constant density, we would prefer to examine the structure of potential vorticity along isopycnals. However, salinity was not measured with the Pegasus instrument, so density cannot be computed. On the anticyclonic side of the Gulf Stream, the T–S relationship is very tight and isopycnals and isotherms are nearly parallel. Figure 2 illustrates the temperature and sigma-θ structure along the Pegasus line from CTD data collected during one of the Pegasus crossings (July 1982).

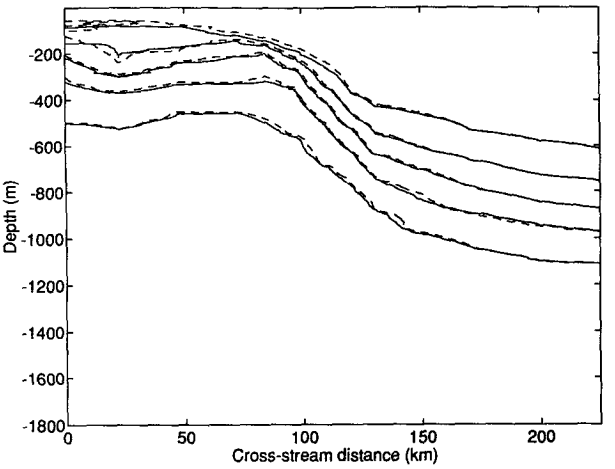

FIG. 2. Contours of temperature (dashed) and sigma-θ (solid) from a CTD section along the Pegasus line in July 1982. Temperature contours (top to bottom) are 17.0, 14.5, 12.0, 9.5, and 7.0°C. Density contours (top to bottom) are 26.58, 26.82, 27.04, 27.23, and 27.51.

The dashed contours show the boundaries of the temperature layers used in the potential vorticity calculations in the main thermocline, and the solid contours are the sigma-θ values, which correspond to these temperatures at the right-hand edge of the section. Because the T–S relationship above 10°C changes across the Gulf Stream, isotherms and isopycnals above this level deviate on the slope water side of the current. Note, however, that the deviations are quite small, on the order of 10 m, which is less than the uncertainty in isotherm depth as measured by the Pegasus instrument. For our purposes, isothermal surfaces are a satisfactory approximation to isopycnal surfaces.

Finally, we consider the isopycnal-following capability of the RAFOS floats. To follow an isopycnal surface exactly, a RAFOS float must have the same compressibility as seawater and be thermally inert (Swift and Riser 1994). The floats used in the Pilot and SYNOP Experiments had compressibilities on the order of 95% (or greater) that of seawater (Song et al. 1994), which means they followed isopycnal surfaces within 0.1 sigma units as they moved along the sloping density surfaces in the Gulf Stream [Swift and Riser 1994, Eq. (3.10)]. The floats also have a nonzero thermal expansion coefficient, which affects their isopycnal-following capability. But because this coefficient is so small, and temperature variations along isopycnals in the main thermocline are also small, the thermal expansion of the floats leads to a negligible isopycnal deviation of only 0.02 sigma units.

The calculated isopycnal deviation of 0.1 sigma units, based on a 95% compressibility, is approximately equivalent to a temperature deviation of 1°C or less along the float trajectories. As will be discussed in the results presented below, this small deviation of floats

from isopycnal surfaces will not significantly impact our results.

d. *The RAFOS launch site*

As mentioned earlier, each float was launched in the same location relative to the thermal structure of the Gulf Stream. Since our analysis depends on this, we have determined how accurately the floats were placed relative to the target location (15°C at 400 m for Pilot, 15°C at 450 m for SYNOP). The XBT profiles made just before each float launch were examined to determine the exact depth of the 15°C isotherm at the launch site. For the SYNOP Experiment, the mean depth of the 15°C isotherm at float deployment was 452 m, with a standard deviation of 22 m. The range was 407 m to 503 m. Using the mean temperature section from the Pegasus study, this standard deviation translates into an rms uncertainty in the cross-stream location of the float launch site of about 3 km. This is quite small compared to the resolution of the Pegasus sections (25 km). The maximum distance away from the target was about 7 km. Not all XBT traces from the Pilot Experiment could be located, but from an examination of about 15, the scatter was of the same order.

3. Results

a. *Basic structure of potential vorticity*

To begin, we describe the synoptic structure of potential vorticity across the Gulf Stream using one example of the 20 Pegasus sections. Figures 3a and 3b show the temperature and downstream velocity cross sections from November 1982. The rectangles superimposed on the sections show that part of the stream seeded with floats in the Pilot (left box) and SYNOP (right box) Experiments. The characteristic warm core of the Gulf Stream is apparent in Fig. 3a, where the maximum temperature exceeds 24°C at the center of the jet near the surface. There is a remnant of the seasonal thermocline capping the thick mode water (18°C) layer on the offshore side of the section. The main thermocline slopes up across the jet with isotherms changing depth by about 500 m. The velocity section, Fig. 3b, indicates maximum speeds of about 180 cm s^{-1}. In Fig. 3c, the velocity section is superimposed on the isotherms that define the layer boundaries in the potential vorticity calculation. The main thermocline, where most of the RAFOS floats were launched, has been divided into four layers between 17° and 7°C.

In Fig. 4, the distributions of layer thickness, relative vorticity, potential vorticity and potential vorticity uncertainty are plotted as a function of temperature and cross-stream distance for November 1982. The mode water layer (17°–19.5°C) is about 300 m thick at the offshore end of the section but thins to less than 50 m across the stream (Fig. 4a). The layers of the main thermocline (7°–17°C) are thinner than the mode water on the offshore side. There is also a minimum in thickness near the center of the jet in these layers. This minimum is observed in several of the sections, but this is the most extreme example. The decreasing stratification below the main thermocline is apparent in the rapid thickening of the layers below 7°C.

In Fig. 4b, the distribution of shear vorticity along isothermal surfaces is shown. There are well-defined regions of positive (cyclonic) and negative (anticyclonic) relative vorticity separated by the jet maximum where relative vorticity goes to zero. The maximum cyclonic vorticity is about 0.4×10^{-5} s^{-1} or about 47% of f, and is found above the main thermocline in the 18°C layer. The maximum anticyclonic vorticity is slightly less, having an absolute value of 0.3×10^{-5} s^{-1} in the warm core near the sea surface.

Minimum values of potential vorticity (Fig. 4c) are coincident with low stratification in the mode water layer and below the main thermocline. As one crosses the stream from right to left, the combined effect of decreasing layer thickness and increasing relative vorticity in the mode water layer leads to a 20-fold increase in potential vorticity. This significant potential vorticity gradient will often be referred to as the potential vorticity front in this work. Below about 14°C, the gradients of potential vorticity are considerably weaker than in the layers above. The midstream maximum results from relatively high stratification (thin layers) near the center of the jet compared to values on either side as seen in Fig. 4a. Note that the uncertainty in potential vorticity (Fig. 4d) is less than 30% in the main thermocline across most of the section.

From the sample section of potential vorticity, it is apparent that the cross-stream structure of potential vorticity changes significantly from the mode water layer through the thermocline layers. Since the RAFOS floats were deployed on various surfaces throughout the main thermocline, we have divided the thermocline into four layers and examined the potential vorticity structure of each layer separately. The floats have also been divided into four groups according to the temperature layer in which they were launched, and the dispersion characteristics for each group have been analyzed separately.

b. *Potential vorticity structure and RAFOS float launch site*

In Figs. 5–8, we present the cross-stream potential vorticity structure (shaded curves) for each of the four layers in the main thermocline: 14.5°–17°C (layer 1, Fig. 5), 12°–14.5°C (layer 2, Fig. 6), 9.5°–12°C (layer 3, Fig. 7), and 7°–9.5°C (layer 4, Fig. 8). In each figure, the 20 panels correspond to the 20 Pegasus sections. Note that sections marked A and B represent two sections taken on the same cruise, usually separated in

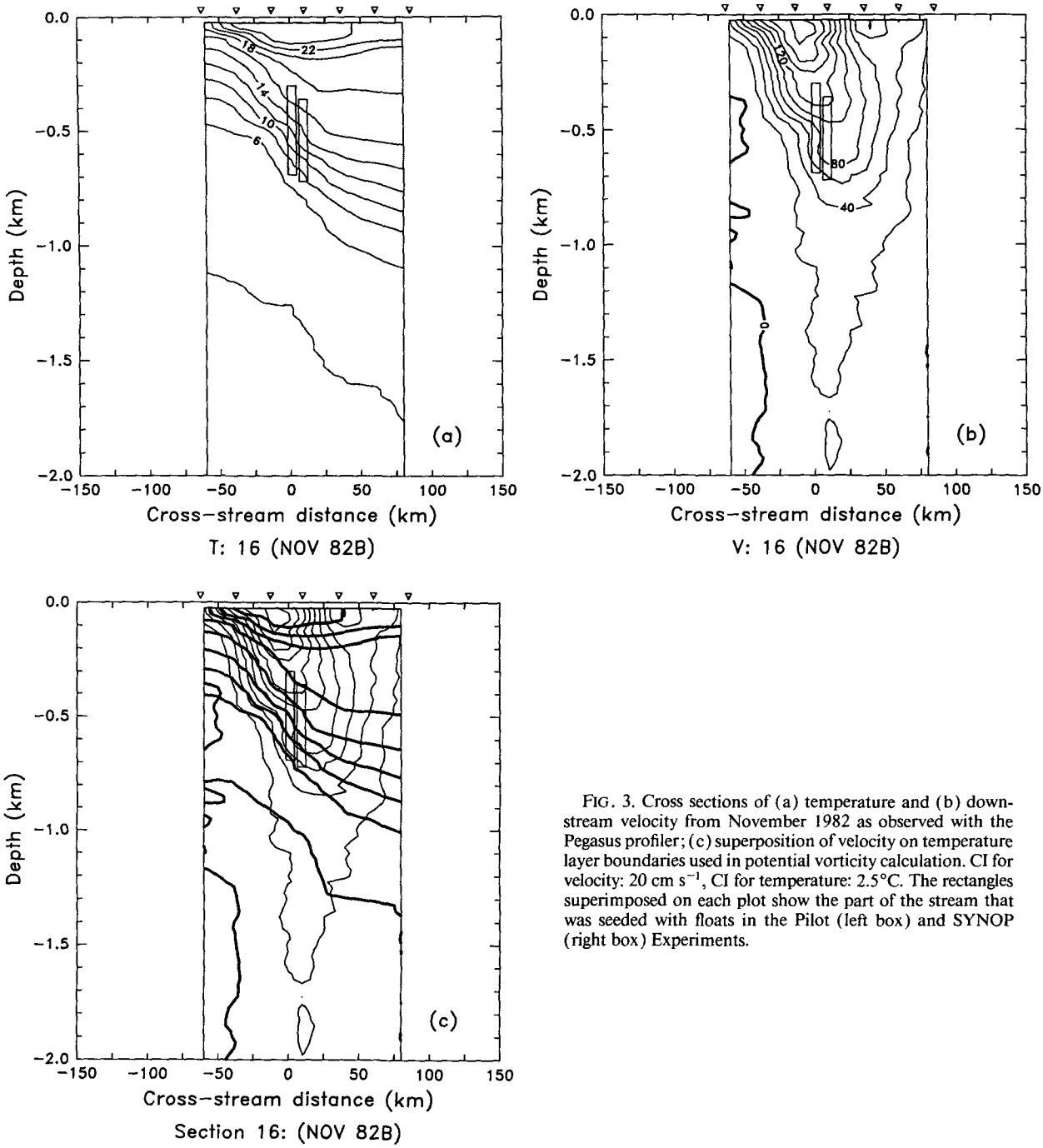

FIG. 3. Cross sections of (a) temperature and (b) downstream velocity from November 1982 as observed with the Pegasus profiler; (c) superposition of velocity on temperature layer boundaries used in potential vorticity calculation. CI for velocity: 20 cm s^{-1}, CI for temperature: 2.5°C. The rectangles superimposed on each plot show the part of the stream that was seeded with floats in the Pilot (left box) and SYNOP (right box) Experiments.

time by about one week. The RAFOS float launch site (or sites) is indicated for each section by a vertical bar 6 km wide, representing the uncertainty in the launch location as described in the methodology, section 2. Floats were deployed in layer 2 during both experiments, so two launch sites are indicated in Fig. 6. The vertically averaged velocity is also shown (solid line) in each panel to illustrate the relationship between the potential vorticity structure and the velocity structure.

In the shallowest layer (Fig. 5) the cross-stream potential vorticity structure is generally characterized by low and uniform potential vorticity on the anticyclonic side of the Gulf Stream. For all the sections except November 1981, which did not cross the entire jet, an increase in potential vorticity is observed on the cyclonic side of the stream. In some cases this increase is part of a local maximum; in other cases, potential vorticity is observed to increase monoton-

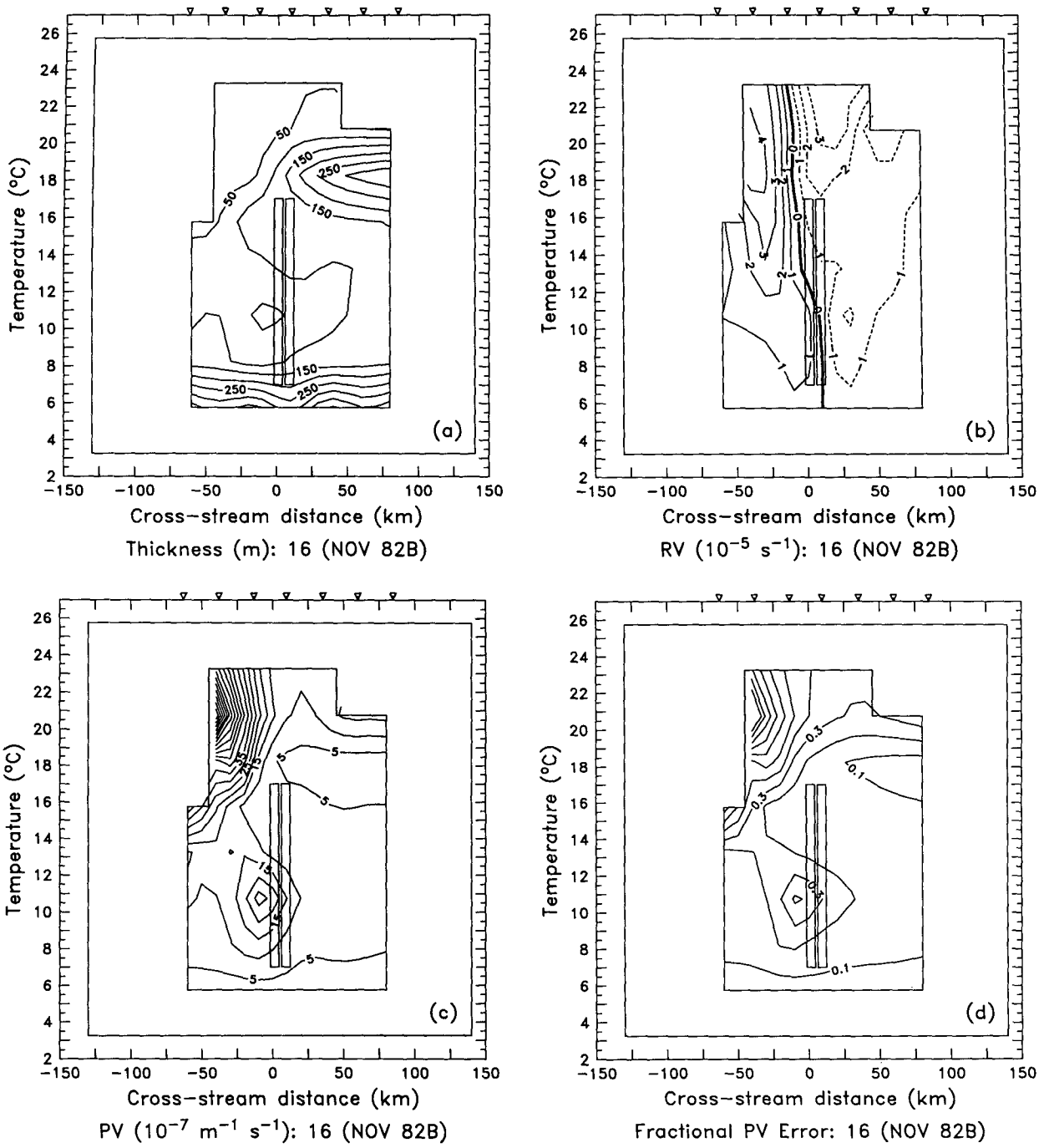

FIG. 4. Cross sections from November 1982 of (a) layer thickness in meters, (b) relative vorticity in 10^{-5} s^{-1}, (c) potential vorticity in 10^{-7} m^{-1} s^{-1}, and (d) uncertainty in potential vorticity expressed as a fraction of potential vorticity. Rectangles are as in Fig. 3.

ically to the left-hand edge of the section. In 17 of the 20 sections, it is clear that the RAFOS float launch site lies offshore of the potential vorticity gradient in water of relatively low potential vorticity. Not including November 1981, the exceptions are March 1981 and March 1983. An inspection of the temperature sections for March 1981 (Fig. 9) indicates that the temperature structure is quite irregular. Due to inclement weather at the time this section and the March 1983 section were made, it took several days to cross the Gulf Stream. The distorted structure observed in Fig. 9 is thought to be the result

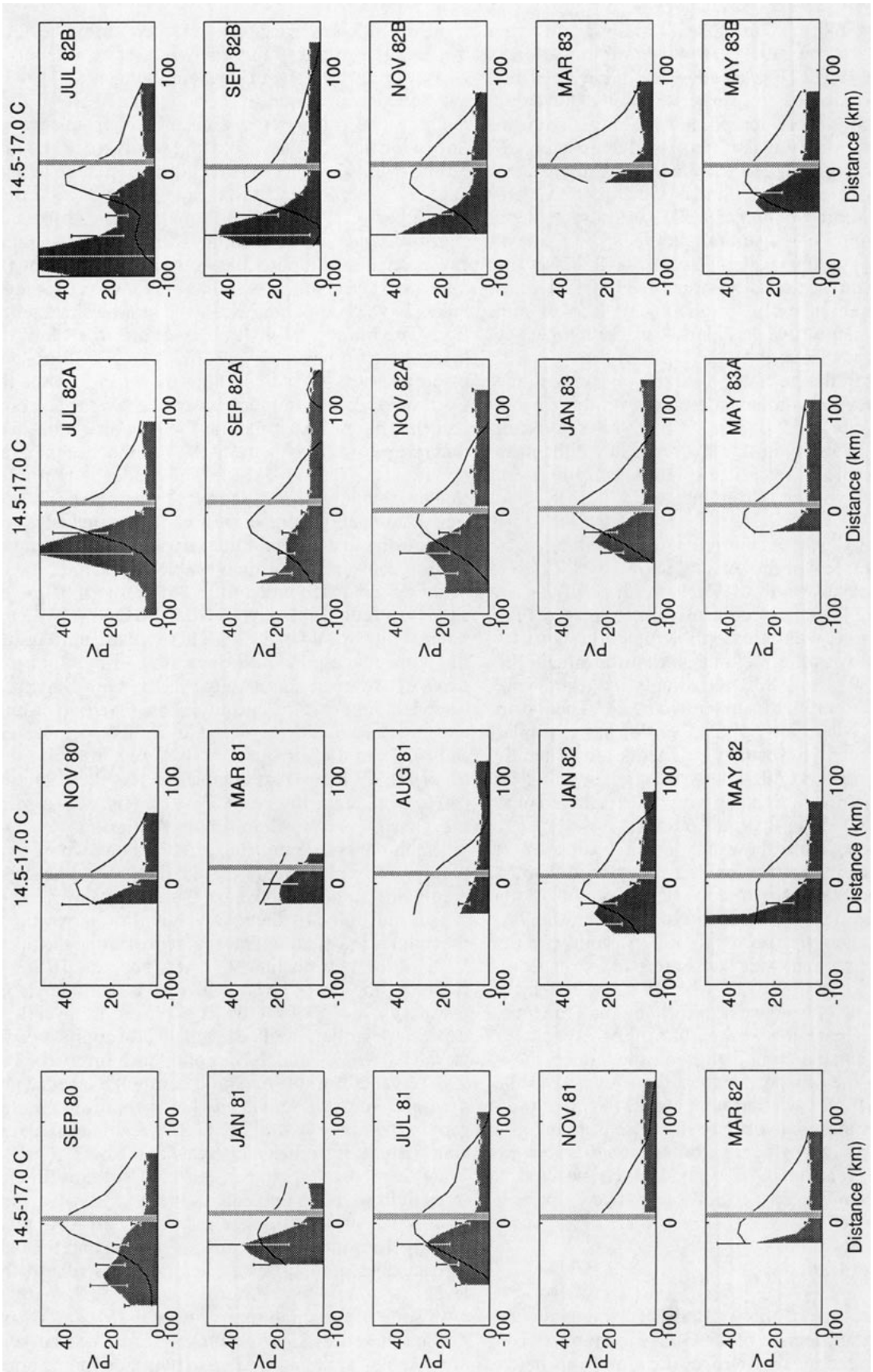

FIG. 5. Cross-stream distribution of potential vorticity, shaded area (in 10^{-7} m^{-1} s^{-1}), and downstream velocity, solid line (in cm s^{-1}, scaled down by a factor of 4) in layer 14.5°–17.0°C for each of the 20 Pegasus sections. The error bars indicate the uncertainty in the estimate of potential vorticity due to uncertainty in the basic observations. The RAFOS float launch site is indicated by the vertical bar. The 6-km width represents the uncertainty in the launch location.

of a shifting of the Gulf Stream path during the crossing (T. Rossby 1993, personal communication).

In the next layer (Fig. 6) the characteristics of the potential vorticity structure are not as well defined due to considerably more temporal variability. Only in about half of the sections is there a well-defined potential vorticity front aligned with the Gulf Stream's cyclonic flank (e.g., July 81, January 82, July 82A, September 82B, and November 82B). In most of these cases, the launch sites again fall on the offshore side of the front, in the low potential vorticity fluid. In the other half of the sections, the structure is characterized by either an absence of a gradient (e.g., May 82 and May 83A), or multiple gradients (e.g., September 80, March 82, and September 82A). From these results, we infer that in the cases when a front *was* present, the RAFOS floats were probably launched on the low potential vorticity side of the front. The significant amount of variability in this layer makes it difficult to be more specific as regards the relationship between the potential vorticity front and the RAFOS float launch site.

In the third layer in the main thermocline, 9.5°–12°C (Fig. 7), few of the sections show a well-defined gradient associated with the cyclonic flank of the jet. The structure is more often nearly uniform across the jet. The sections with a discernible potential vorticity front aligned with the cyclonic side of the stream are September 82A and 82B. Gradients in general are much weaker than in the upper two layers. The fourth and deepest layer, 7°–9.5°C (Fig. 8), has a similar character. Potential vorticity gradients are generally weak if they exist at all. The weak gradients that do exist are sometimes associated with midstream maxima such as in September 80 and January 83.

In sum, these results show that only in the uppermost layer of the main thermocline is a strong, well-defined potential vorticity gradient consistently present along the Gulf Stream's cyclonic flank. In this layer, the RAFOS float launch site appears to be consistently on the low potential vorticity side (offshore side) of the front. In the next layer down, 12°–14.5°C, a well-defined potential vorticity front exists only about half the time, and when it is there, it is weaker than in the layer above. In the cases when a front is present, the launch site is generally on the low potential vorticity side, as in the layer above. In the two bottom layers of the main thermocline, the potential vorticity structure is more aptly characterized as being nearly homogeneous across the jet. In these layers, the RAFOS float launch site appears to be in the middle of a region of relatively uniform potential vorticity.

c. *RAFOS float dispersion statistics*

The trajectories of the 95 RAFOS floats launched in the main thermocline of the Gulf Stream have been compared to sea surface temperature maps to determine if and how each float escaped from the Gulf Stream. The results of this analysis have been reported by Bower and Rossby (1989) and Song et al. (1993). We have consolidated the results from these studies, defining two categories of escape mechanism: escape due to formation of new cold and warm core rings and escape by means *other* than the formation of new rings. We have also collated the escape statistics according to temperature. Table 1 summarizes the dispersion statistics, and Fig. 10 illustrates the results schematically. Because the potential vorticity structure in the lower two layers was very similar, the statistics for these layers have been combined in the graphical presentation. The number of float observations in each of the layers is very uneven; layer 2 (12°–14.5°C) was sampled most heavily, with 51 float trajectories, while the top layer and the combined lower two layers had about half that many. In estimating the proportion of floats that escape, we have included 95% confidence intervals (Iman and Conover 1983). The reader is reminded that the small number of samples renders some of these statistical results more suggestive than conclusive.

Focusing first on the statistics for all the floats taken as one group (last column of Table 1), we find that 69 of the 95 floats launched in the main thermocline escaped from the stream in less than 30 days (73%, confidence interval 64%–82%). This statistic emphasizes the point made previously that most of the fluid particles in the main thermocline of the Gulf Stream at Cape Hatteras exit the current in less than one month, and are presumably replaced by other particles entrained from the surrounding fluid. We also find that 62 of the 69 floats that escaped in less than 30 days (90%, confidence interval 83%–97%) did so via some mechanism(s) *other* than ring formation.

When the escape statistics are broken down by temperature layer, it is found that floats in the upper layer are retained longer on average than in the lower layers. This is illustrated by the relatively minor narrowing of the main arrow shaft in Fig. 10a, representing the upper layer of the thermocline (cf. Figs. 10b and 10c) representing the lower layers. Only 40% (confidence interval 19%–64%) of the floats deployed in layer 1 escaped in less than 30 days, while 82% (confidence interval 71%–93%) and 79% (confidence interval 63%–95%) escaped from layer 2 and combined layers 3 and 4, respectively. These statistics lend support to the concept of the upper part of the Gulf Stream as a Lagrangian current, introduced by Shaw and Rossby (1984). They defined a Lagrangian current as a current that traps fluid particles and carries them far downstream. In the deep main thermocline, floats are lost more quickly from the Gulf Stream, suggesting that the Gulf Stream does not exist as a Lagrangian current at this level.

In spite of the small sample sizes in layers 1, 3, and 4, the differences in *direction* of escape in each layer are notable. Losses were equal to both sides in the upper

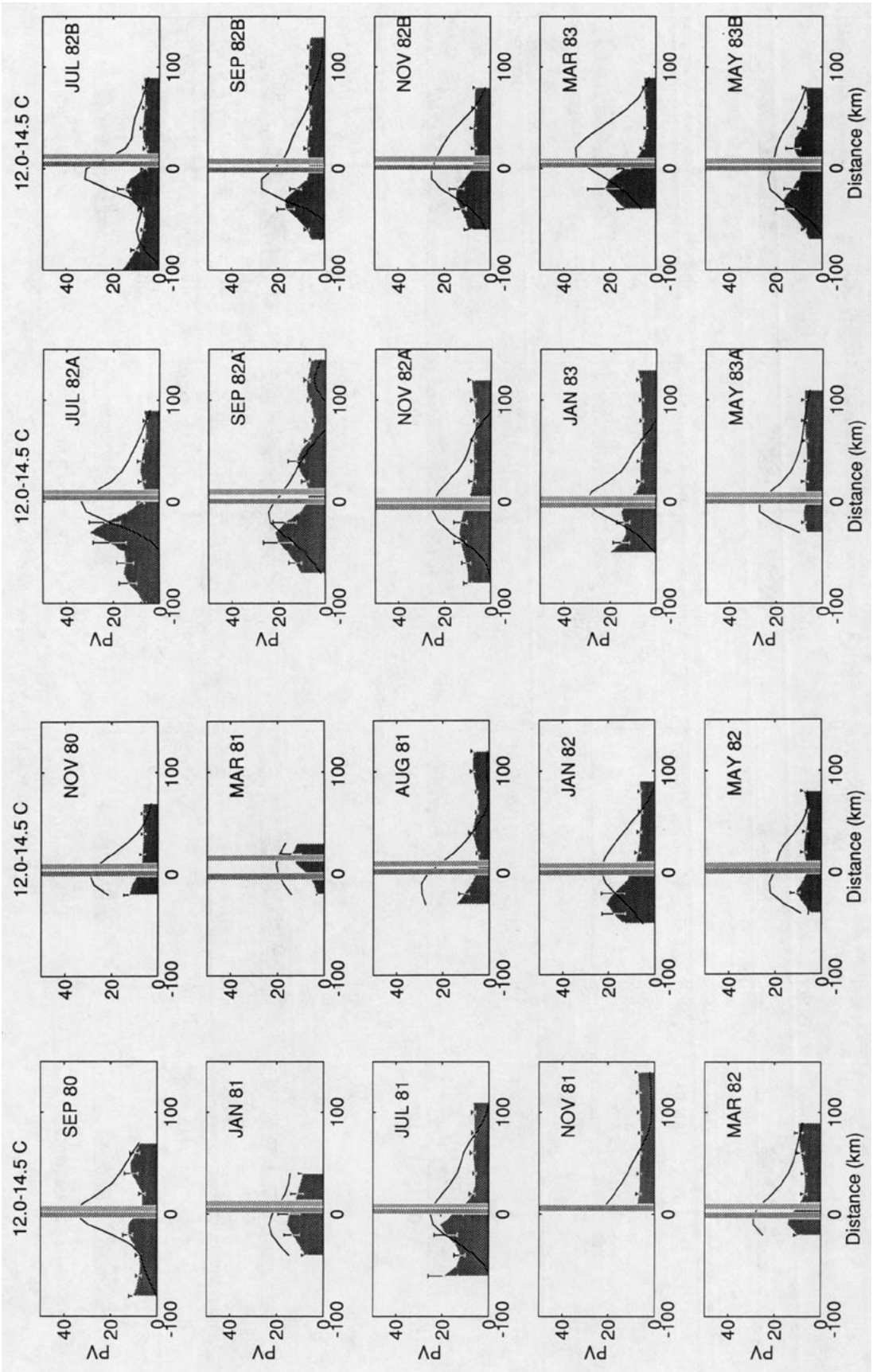

FIG. 6. Same as in Fig. 5 but for layer 12.0°–14.5°C. Floats were deployed in this layer during both experiments, so two launch sites are indicated.

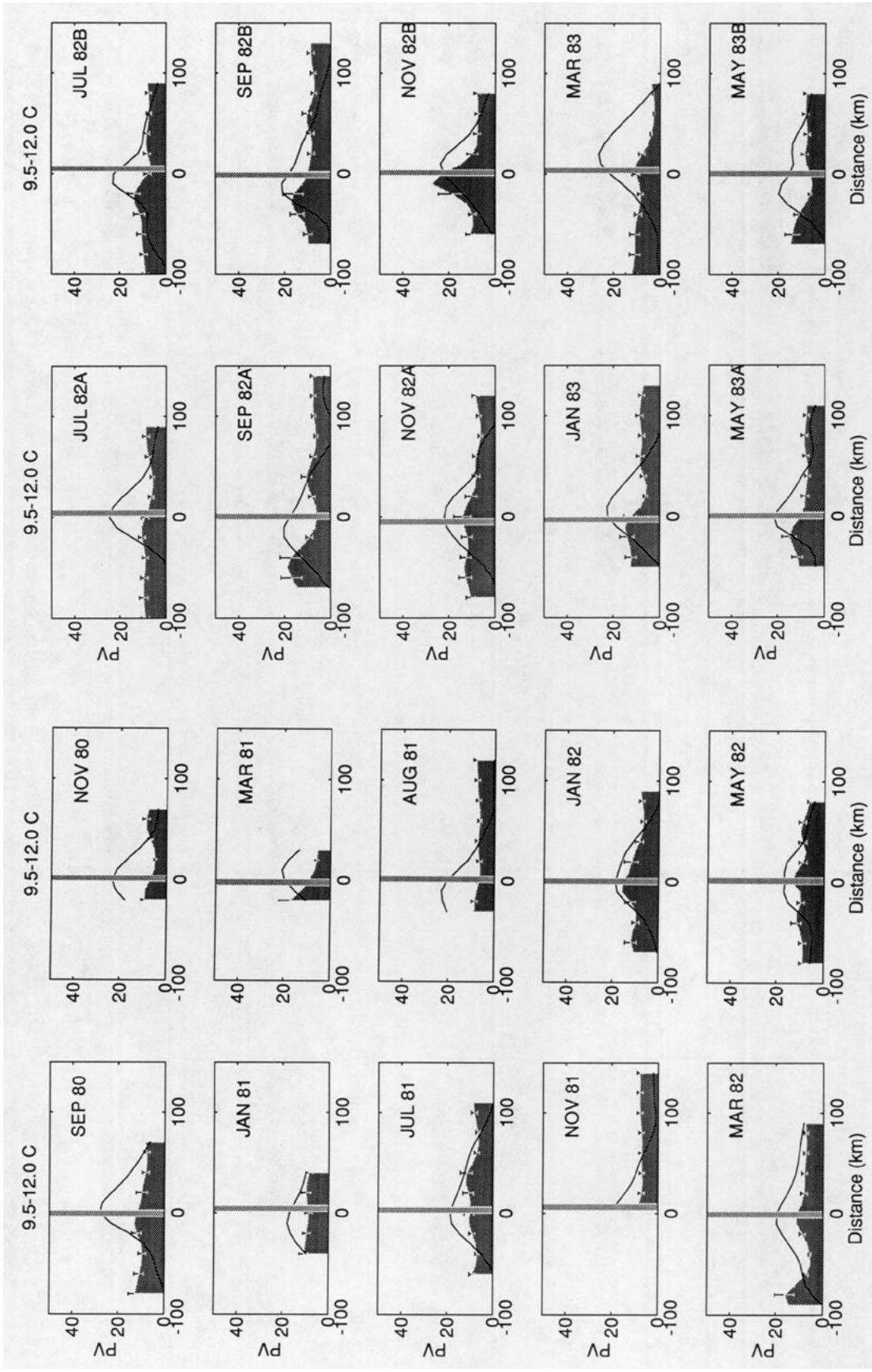

FIG. 7. Same as in Fig. 5 but for layer 9.5°–12.0°C.

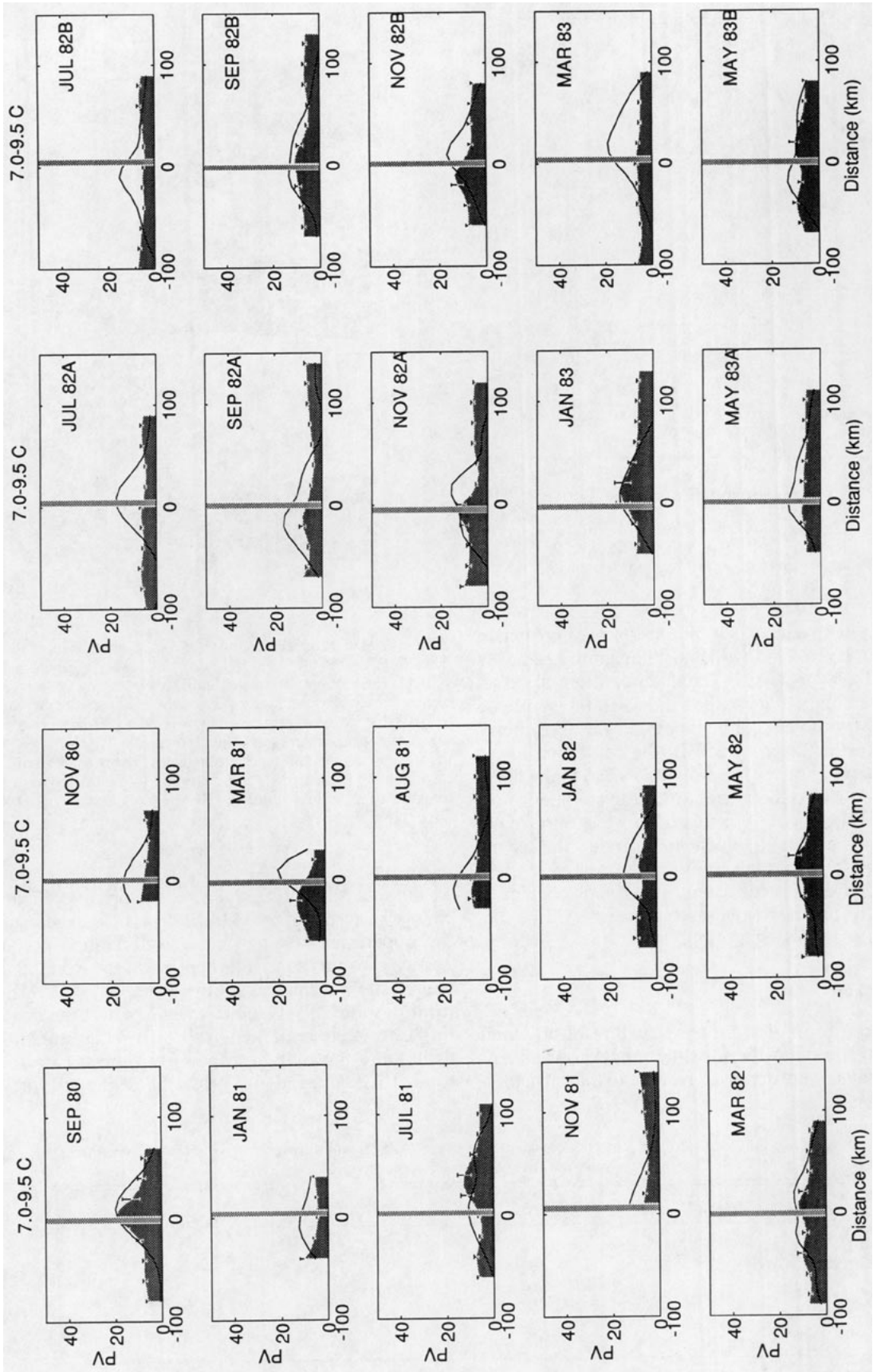

FIG. 8. Same as in Fig. 5 but for layer 7.0°–9.5°C.

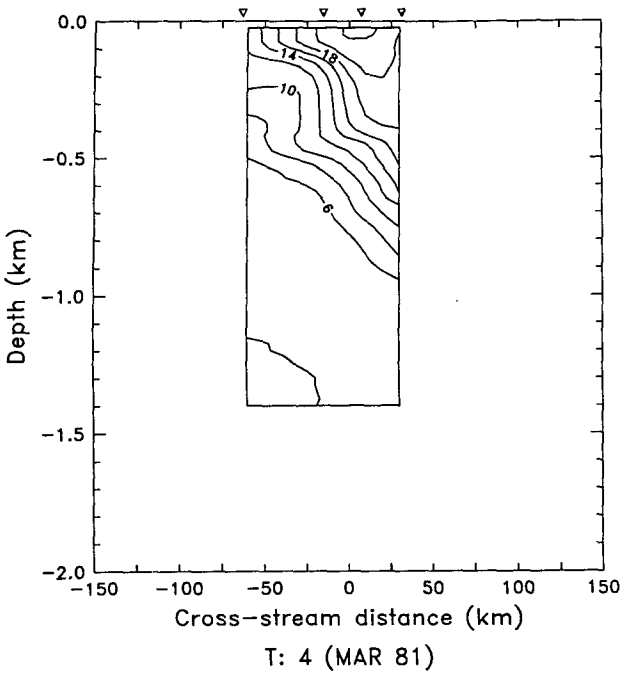

FIG. 9. Cross section of temperature for March 1981.

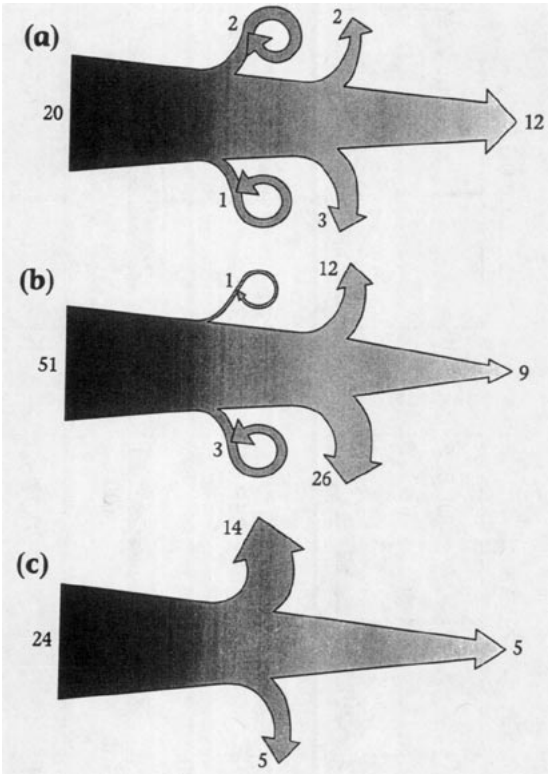

FIG. 10. Schematic representation of dispersion statistics of RAFOS floats in layers (a) 14.5°–17.0°C, (b) 12.0°–14.5°C, and (c) 7.0°–12.0°C. The numbers on the left indicate how many floats were deployed in each layer, and the values on the right indicate the number of floats that stayed in the stream for more than 30 days. The arrows shown leaving the main arrow shaft indicate floats that escaped from the stream via rings and other mechanisms. The more dramatic narrowing of the main arrow shaft in (b) and (c) compared to (a) represents the greater loss of floats in the deeper layers compared to the upper layer.

layer (4 floats to each side), but losses were greater to the south in layer 2 and to the north in combined layers 3 and 4. In layer 2, 69% (confidence interval 55%–84%) of the floats that escaped did so to the south, so we can say (with 95% confidence) that the asymmetry observed in this layer is real. In the combined lower layers, 74% (confidence interval 48%–92%) of the floats that escaped left to the north. Since the confidence interval drops below 50% in this case, we cannot make statistically significant conclusions about the asymmetry at this level, but the asymmetry observed in these layers, and layer 2, is consistent with the placement of floats relative to the velocity structure, as will be discussed in the following section.

4. Discussion

With the information on the structure of potential vorticity in the main thermocline, and knowledge of where the floats were deployed relative to that structure, we are in a position to interpret the observed float exchange in terms of cross-frontal particle exchange. In the uppermost layer, where a well-defined potential vorticity front is consistently present, the RAFOS float launch site was located south of the potential vorticity front in water of subtropical origin. Thus, the floats in this layer that remained trapped in the stream (12 floats) and those that escaped from the stream to the south (4 floats) did not cross the potential vorticity

TABLE 1. Dispersion statistics for RAFOS floats deployed in the Gulf Stream during the RAFOS Pilot Experiment and the RAFOS SYNOP Experiment.

Category	7.0°–9.5°C	9.5°–12.0°C	12.0°–14.5°C	14.5°–17.0°C	Total
Nonring (north)	9	5	12	2	28
Nonring (south)	2	3	26	3	34
Ring (north)	0	0	1	2	3
Ring (south)	0	0	3	1	4
Retained	3	2	9	12	26
Total	14	10	51	20	95

front. It is only the four floats that escaped from the stream to the *north* that apparently crossed the potential vorticity front. We will return to a more detailed description of these four trajectories later.

Skipping to the lower two layers, it was shown that a strong potential vorticity gradient is not present at this level. The large dispersion of RAFOS floats to the north and south at this level is indicative of significant *particle* exchange between the Gulf Stream and the surrounding fluid, but this particle exchange is taking place in a relatively homogeneous pool.

It is more difficult to draw definitive conclusions from the results for layer 2, where we observed substantial temporal variability in the potential vorticity structure. Based on the observation that the float launch site is located south of the potential vorticity front when one exists, we conclude that much of the significant loss of floats to the south is probably representative of fluid particles recirculating within the same water mass south of the Gulf Stream. We note here that because the floats have been analyzed in 2.5°C bins and because the maximum error of temperature drift is 1°C, the second layer essentially acts as a buffer zone to accommodate this error. Thus, floats initially launched in the upper layer would not have drifted into the lower two layers and vice versa. Because our major distinction is between the float behavior in the upper layer versus float behavior in the lower two layers, having the second layer act as an error "buffer" does not seriously degrade our interpretation. Also, we note that although the maximum calculated drift is 1°C (which matches the observed maximum range), the actual temperature difference between the float temperature at the time of launch and the time of escape was, on average, only 0.24°C. Because this temperature difference is one order of magnitude less than the range of the temperature bins, with this measure of error we are even more certain that floats did not cross from one isothermal layer to another.

The striking asymmetry in float escape in layer 2 and in the lower two layers is an intriguing feature (Fig. 10). It appears to be related to the placement of the floats with respect to the velocity structure of the jet. Figures 5–8 and Fig. 4b show that as one moves down through the water column, the maximum in downstream velocity decreases and shifts to the right. This means the float launch site, which is on the anticyclonic side in the upper layers, falls increasingly on the cyclonic side of the stream with increasing depth. So floats launched in layer 2, which had a tendency to escape to the south, were most likely launched on the anticyclonic side of the jet maximum, and floats deployed deeper in the main thermocline, which were lost preferentially to the north, were placed on the cyclonic side. This pattern is consistent with the kinematic model results of Bower (1991), who showed that particles on the anticyclonic side of the stream will most likely be lost to the south, and particles on the cyclonic side are more likely to escape from the current to the north, due to phase propagation of meanders. The floats in layer 1 do not exhibit any asymmetry, and they also have the highest retention rate of all the layers (Fig. 11). This suggests that the downstream velocity in this layer is high enough compared to the phase speed of meanders that these floats are trapped more effectively than in the lower layers.

To guide our interpretation of the observed pattern of particle exchange in the Gulf Stream, we have considered the results from a study of particle behavior in a quasigeostrophic EGCM by Lozier and Riser (1990). The EGCM used by Lozier and Riser was a square ocean model, with no topography and with a steady wind pattern that produces two antisymmetrical gyres. Obviously these features severely restrict this model's applicability to the Gulf Stream. However, this model does have a depth-dependent potential vorticity front aligned with its extended western boundary current, as does the Gulf Stream. Thus, we can compare the patterns of exchange in the vicinity of potential vorticity gradients. In this regard the model is used to study a process, namely, particle exchange.

In the top layer of the model used by Lozier and Riser, a strong, narrow potential vorticity front is embedded in the midlatitude jet (mean streamfunction and potential vorticity fields shown in Fig. 12). Figure 13a illustrates the 45-day trajectories of 16 model floats initiated simultaneously in the potential vorticity front along the western boundary in the northern gyre. All the floats remain trapped in the midlatitude jet, not crossing into the southern gyre until the jet disintegrates

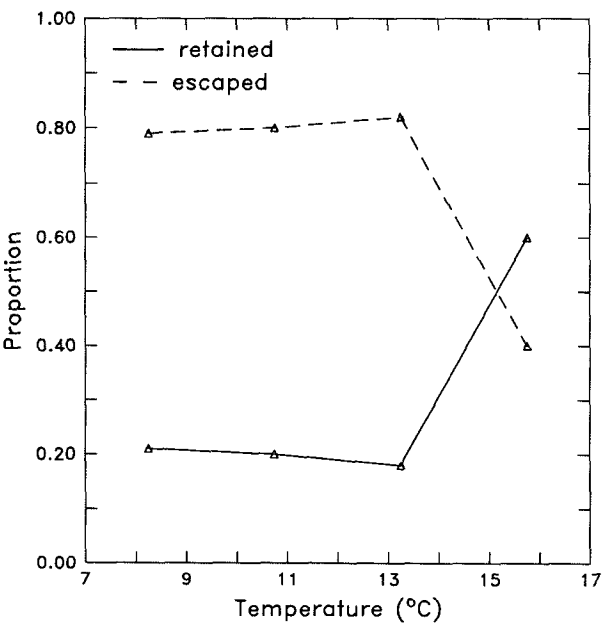

FIG. 11. Retention/escape proportions of RAFOS floats in the main thermocline of the Gulf Stream as a function of temperature.

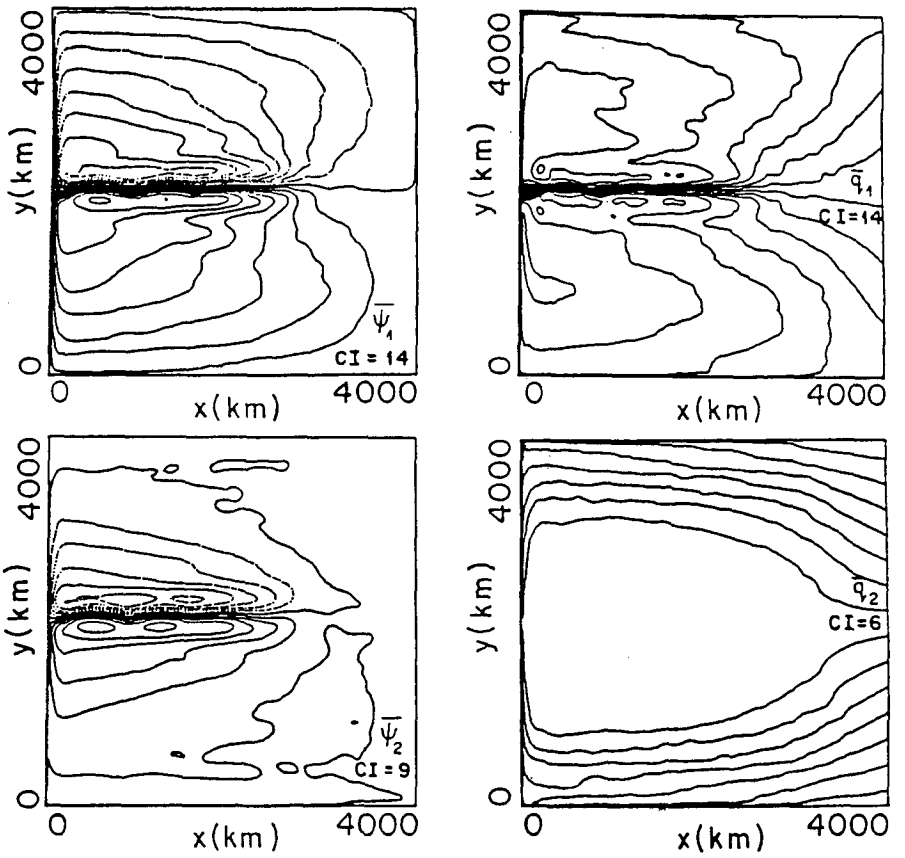

FIG. 12. Mean streamfunction and mean potential vorticity distribution in the top and middle layer of the three-layer, wind-driven, quasigeostrophic EGCM studied by Lozier and Riser (1989, 1990). CI for the streamfunction fields is 10^{-3} m^2 s^{-1} and CI for the potential vorticity fields is $100/f_0$.

into eddies near the eastern boundary (cf. with Fig. 12). In this particular case, all 16 floats crossed into the southern gyre at the jet exit, but in other realizations, particles returned to the northern gyre or were split between the gyres. In Fig. 13b, 16 trajectories of model floats released across the width of the midlatitude jet, but on the northern side of the potential vorticity front, are shown. In this case, particles escape from the jet more quickly, yet they only recirculate within their gyre of origin (northern gyre). None crossed the jet into the southern gyre until the jet breaks up, as in the other setting. Although it is not indicated in these sample trajectories, some floats did cross from one gyre to the other during the formation of rings.

We also show the results from layer 2 of the model, which is isolated from surface forcing. At this level, the midlatitude jet is embedded in a region of relatively uniform potential vorticity (Fig. 12). Model floats initiated in this layer at the same location as in Figs. 13a and 13b appear to escape from the midlatitude jet farther upstream than their counterparts in the upper layer, as shown in Figs. 13c and 13d. Based on an analysis of these and thousands of other "floats," Lozier and Riser concluded that potential vorticity was a dominant constraint on flow paths and that particle exchange was very sensitive to the position of the float launch relative to the potential vorticity front.

The pattern of particle exchange observed with the RAFOS floats is similar to that seen in the model. In the upper main thermocline, where a strong potential vorticity front is present, particle exchange across the front is extremely limited. Some particles are exchanged with the surrounding fluid, but they generally stay on the same side of the front. In the deep main thermocline, significant particle exchange is observed between the Gulf Stream and fluid on both sides of the jet, where there is no potential vorticity front at this level.

We now consider the trajectories of the four RAFOS floats that apparently did cross the potential vorticity front in hopes of identifying what mechanisms contribute to cross-frontal particle exchange. In Figs. 14a and 14b, it can be seen that RAFOS 133 and RAFOS 138 clearly escaped from the stream during the formation of new warm core rings. This is apparent from the anticyclonic rotation of the trajectories. In the convolution of the Gulf Stream path that results in the

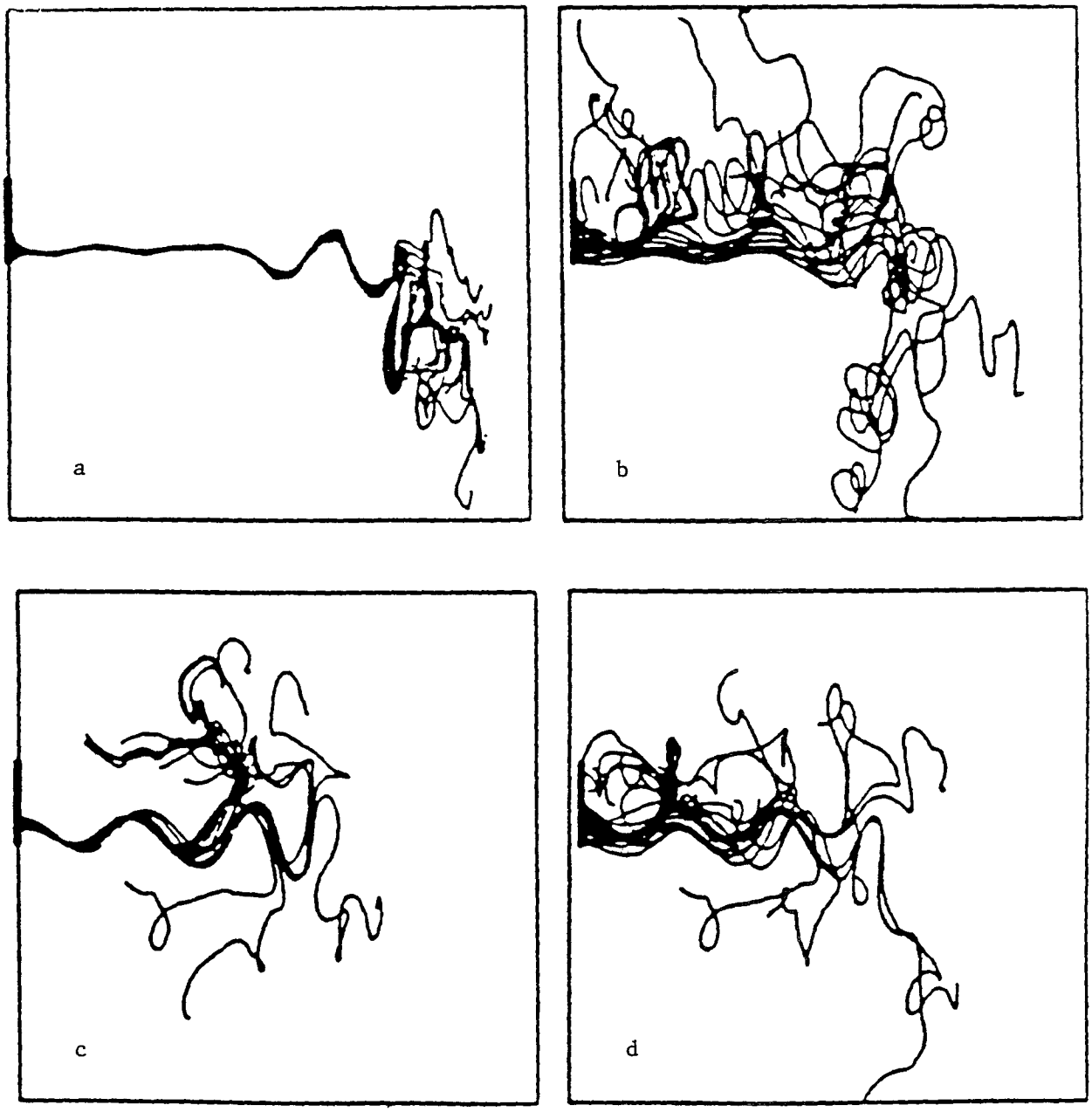

FIG. 13. (a) The 45-day trajectories of 16 "floats" initiated in the narrow potential vorticity front of the northern gyre in the top layer of a quasigeostrophic EGCM; (b) as in (a) but with initial float location spanning the entire width of the extended boundary current in the northern gyre; (c) trajectories of 16 model floats initiated at the same location as in (a) but in the second layer; (d) trajectories of 16 model floats initiated in the same location as (b) but in the second layer.

formation of a warm core ring, the potential vorticity front is similarly convoluted and pinches off, enclosing a core of low potential vorticity fluid. Particle exchange via ring formation was also seen in the model trajectories, so this behavior appears to be compatible with that of the model floats.

Figure 14c shows the trajectory of RAFOS 127, which escaped from the stream near 53°W, on about yesterday 235, 1988. Its escape from the stream is indicated by the rapid deceleration prior to day 235, the reversal in flow direction after day 235, and the shoaling of the float as indicated in its pressure record (Fig. 15a). The fluid particle tagged by the float apparently moved up the sloping density surface into the region north of the stream. Subsequent reentrainment is indicated by the acceleration of the float and downwelling. The float does not appear to have been caught in the formation of a new ring,

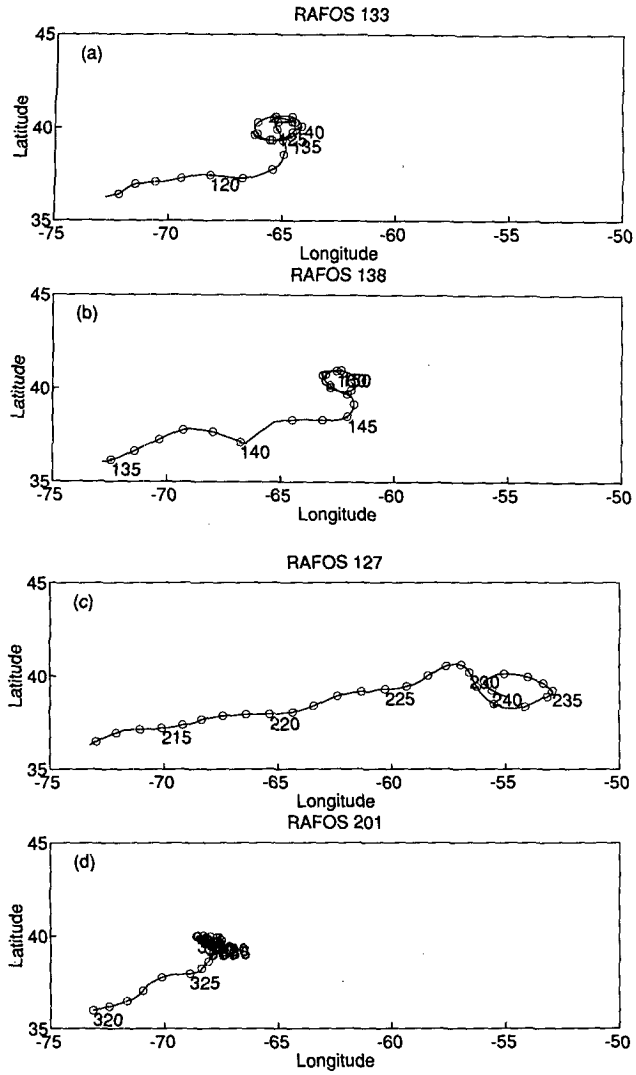

FIG. 14. Trajectories of four RAFOS floats from the upper layer that escaped from the Gulf Stream to the north. (a) RAFOS 133; (b) RAFOS 138; (c) RAFOS 127; (d) RAFOS 201. Open circles denote daily positions with every fifth day marked.

but large amplitude looping of the jet is apparent in this area.

This behavior was also exhibited by many of the floats in the upper layer of the QG model. As shown in Figs. 13a and 13b, model floats in the top layer often escaped from the midlatitude jet near the jet exit, where there is no longer a strong potential vorticity front associated with the jet. There is some evidence that by 53°W, the cross-stream property gradients in the main thermocline of the Gulf Stream have also been weakened. Bower et al. (1985) noted a weakening of the cross-stream dissolved oxygen gradient with increasing downstream distance at this level, and Hall and Fofonoff's (1993) comparison of the potential vorticity structure at 68° and 55°W indicates a decrease in the cross-stream gradient at this level. So this float may not have actually crossed a front as it escaped from the Gulf Stream to the north, but rather left the stream at a point where the potential vorticity front was substantially weakened.

RAFOS 201, shown in Fig. 14d, is perhaps the most interesting of the four trajectories shown here because it escaped from the stream to the north rather quickly, in less than 10 days, and it does not appear to have been caught in the formation of a new ring. The process leading to the escape of this float is not known, but we note that it is accompanied by a rapid shoaling: between days 326 and 332, the float rose about 450 m as illustrated in Fig. 15b. This corresponds to an average vertical velocity of 0.09 cm s^{-1} and a horizontal divergence of

$$\frac{\partial w}{\partial z} \approx \frac{W}{H} = 1.8 \times 10^{-6}\ \mathrm{s}^{-1},$$

assuming a vertical length scale of 500 m. In the quasi-geostrophic approximation, the horizontal divergence is on the order of

$$\frac{\partial w}{\partial z} = \epsilon\left(\frac{\partial u}{\partial x}, \frac{\partial v}{\partial y}\right) \approx \epsilon\left(\frac{U}{L_x}, \frac{V}{L_y}\right)$$

or

$$\epsilon = \left(\frac{WL_x}{UH}, \frac{WL_y}{VH}\right),$$

where ϵ is the Rossby number. Using $W = 0.1$ cm s^{-1}, $L_x = 50$ km, $U = 10$ cm s^{-1}, and $H = 500$ m, the Rossby number is O(1). This suggests that whatever process is acting to cause RAFOS 201 to cross out of the stream to the north, it is one that violates the quasi-

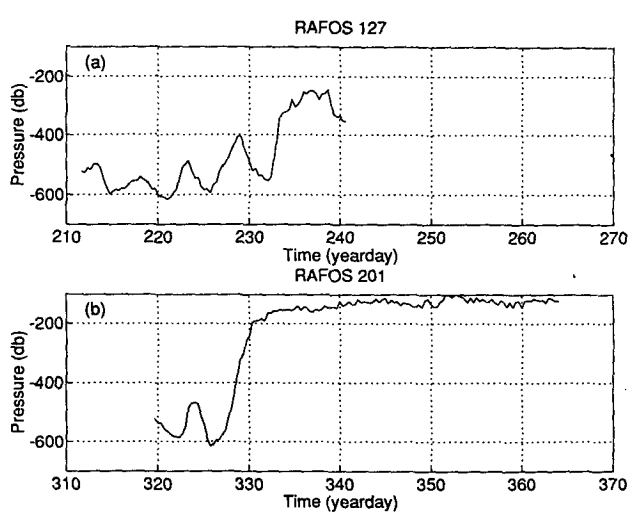

FIG. 15. Pressure records for (a) RAFOS 127 and (b) RAFOS 201 as a function of time.

geostrophic approximation, and therefore we do not expect to see it manifested in the trajectories of the model floats.

It appears that the model trajectories in the top layer of the QG EGCM studied by Lozier and Riser (1990) are generally compatible with observations of particle motion in the Gulf Stream. In both cases, the strong potential vorticity front associated with the midlatitude jet appears to restrict particles from crossing out of the stream. Some cross-frontal particle exchange is achieved in the Gulf Stream by means of ring formation, and this process is also represented in the model. There is evidence based on one float trajectory that ageostrophic processes that are not present in the model may contribute to particle and property exchange in the Gulf Stream. Obviously, this cross-frontal exchange process needs further study before it can be considered as an important mechanism in particle exchange across the Gulf Stream.

5. Summary

In this study we have examined the extent to which float exchange between the Gulf Stream and the surrounding fluid is indicative of cross-frontal particle exchange. Our first task was to determine where RAFOS floats deployed in the Gulf Stream have typically been launched relative to the potential vorticity structure of the jet. We used velocity and temperature sections made across the Gulf Stream near the RAFOS float launch location northeast of Cape Hatteras to construct sections of potential vorticity in isothermal coordinates. The cross-stream structure of potential vorticity was found to be depth dependent through the main thermocline, so the structure was examined in four layers between 17° and 7°C. The RAFOS float dispersion statistics were also classified based on the mean temperature along their tracks.

It was found that in the upper layer of the main thermocline, a strong, well-defined potential vorticity front is consistently present and aligned with the cyclonic side of the Gulf Stream. Furthermore, it was demonstrated that the RAFOS float launch site was on the offshore side of this front, in low potential vorticity water of subtropical origin. Based on this result, it was determined that only three isopycnal floats in the upper layer (3% of all floats launched in the main thermocline) actually crossed the potential vorticity front at this level. The remainder either stayed in the stream for a considerable distance or escaped to the south: in either case, these floats did not cross the front.

In the second layer, a well-defined potential vorticity front was present only about half the time. When a front was present, it was weaker than the front in the upper layer, and the float launch site was usually on the low potential vorticity side of the front. Because of the significant temporal variability observed in this layer, it was more difficult to draw general conclusions regarding the interpretation of particle dispersion in this layer. However, we have speculated that much of the particle exchange to the south observed in this layer is representative of fluid particles recirculating within their gyre of origin. In the lower two layers of the main thermocline, the potential vorticity distribution is quite uniform. The large amount of particle exchange observed in these layers is therefore representative of fluid particles circulating within a pool of relatively homogeneous fluid.

These characteristics of particle motion are generally compatible with the cross-frontal particle exchange patterns found within a QG EGCM by Lozier and Riser (1990). The fact that the QG model does a reasonable job of reproducing the basic patterns of particle exchange in the Gulf Stream is an encouraging result. Direct observations of particle motion are invaluable for determining flow patterns over a broad geographical area, but there are rarely enough synoptic hydrographic observations accompanying the trajectories to relate particle exchange directly to cross-frontal property fluxes. A dynamical description of the processes leading to the dispersion is also difficult to capture from the trajectories alone. Models can provide information on the flow field within which the particles are embedded, making dynamical analysis possible, as demonstrated by Lozier and Riser (1990). There is some evidence presented here that suggests higher-order dynamics may more accurately reproduce some aspects of particle motion in midlatitude jets. Better resolution will also undoubtably reveal more details of the particle exchange.

Acknowledgments. We are grateful to T. Song and T. Rossby of the University of Rhode Island for their willingness to share the trajectory analysis results from the SYNOP RAFOS experiment prior to publication. We also thank M. McCartney and R. Samelson for valuable comments and suggestions, and B. Owens for help in the initiation of this project. This work was supported by the Office of Naval Research under Grant No. N00014-91-J-1425.

REFERENCES

Anderson-Fontana, S., and T. Rossby, 1991: RAFOS Floats in the SYNOP Experiment: 1988–1990. University of Rhode Island Tech. Report, Ref. 91-7, 155 pp.

Bower, A. S., 1989: Potential vorticity balances and horizontal divergence along particle trajectories in Gulf Stream meanders east of Cape Hatteras. *J. Phys. Oceanogr.*, **19**, 1669–1681.

——, 1991: A simple kinematic mechanism for mixing fluid parcels across a meandering jet. *J. Phys. Oceanogr.*, **21**, 173–180.

——, and T. Rossby, 1989: Evidence of cross-frontal exchange processes in the Gulf Stream based on isopycnal RAFOS float data. *J. Phys. Oceanogr.*, **19**, 1177–1190.

——, ——, and J. L. Lillibridge, 1985: The Gulf Stream—Barrier or blender. *J. Phys. Oceanogr.*, **15**, 24–32.

——, ——, and R. O'Gara, 1986: RAFOS Float Pilot Studies in the Gulf Stream. University of Rhode Island Tech. Report, Ref. 86-7, 110 pp.

Csanady, G. T., 1989: Energy dissipation and upwelling in western boundary currents. *J. Phys. Oceanogr.*, **19,** 462–473.

Cushman-Roisin, B., 1993: Trajectories in Gulf Stream meanders. *J. Geophys. Res.*, **98,** 2543–2554.

Ertel, H., 1942: Ein neuer hydrodynamischer Wirbelsatz. *Meteor. Z.*, **59,** 277–282.

Fuglister, F. C., 1963: Gulf Stream '60. *Progress in Oceanography,* Vol. 1, Pergamon, 265–373.

Halkin, D., and T. Rossby, 1985: The structure and transport of the Gulf Stream at 73°W. *J. Phys. Oceanogr.*, **15,** 1439–1452.

Hall, M. M., and N. P. Fofonoff, 1993: Downstream development of the Gulf Stream from 68°W to 55°W. *J. Phys. Oceanogr.*, **23,** 225–249.

Harrison, D. E., and W. R. Holland, 1981: Regional eddy vorticity transport and the equilibrium vorticity budgets of a numerical model ocean circulation. *J. Phys. Oceanogr.*, **11,** 190–208.

Hogg, N. G., 1992: On the transport of the Gulf Stream between Cape Hatteras and the Grand Banks. *Deep-Sea Research,* **39,** 1231–1246.

Holland, W. R., and P. B. Rhines, 1980: An example of eddy-induced ocean circulation. *J. Phys. Oceanogr.*, **10,** 1010–1031.

Iman, R. L., and W. J. Conover, 1983: *A Modern Approach to Statistics.* John Wiley and Sons, 497 pp.

Leaman, K. D., E. Johns, and T. Rossby, 1989: The average distribution of volume transport and potential vorticity with temperature at three sections across the Gulf Stream. *J. Phys. Oceanogr.*, **19,** 36–51.

Lozier, M. S., and S. C. Riser, 1989: Potential vorticity dynamics of western boundary currents in a quasi-geostrophic ocean. *J. Phys. Oceanogr.*, **19,** 1373–1396.

——, and ——, 1990: Potential vorticity sources and sinks in a quasi-geostrophic ocean: beyond western boundary currents. *J. Phys. Oceanogr.*, **20,** 1608–1627.

McDowell, S., P. Rhines, and T. Keffer, 1982: North Atlantic potential vorticity and its relation to the general circulation. *J. Phys. Oceanogr.*, **12,** 1417–1436.

Owens, W. B., 1984: A synoptic and statistical description of the Gulf Stream and subtropical gyre using SOFAR floats. *J. Phys. Oceanogr.*, **14,** 104–113.

Press, W. H., B. P. Flannery, S. A. Teukolsky, and W. T. Vetterling, 1988: *Numerical Recipes in C.* Cambridge University Press, 735 pp.

Shaw, P.-T., and H. T. Rossby, 1984: Toward a Lagrangian description of the Gulf Stream. *J. Phys. Oceanogr.*, **14,** 528–540.

Song, T., T. Rossby, and E. Carter, 1994: Lagrangian studies of fluid exchange between the Gulf Stream and surrounding waters. *J. Phys. Oceanogr.*, submitted.

Swift, D. D., and S. C. Riser, 1994: RAFOS floats: Defining and targeting surfaces of neutral buoyancy. *J. Atmos. Oceanic Technol.*, in press.

Worthington, L. V., 1976: On the North Atlantic Circulation. *Johns Hopkins Oceanographic Studies,* No. 6, 110 pp.